J|A|C|S COMMUNICATIONS

Published on Web 10/13/2010

Unusual Inverse Temperature Dependence on Reaction Rate in the Asymmetric Autocatalytic Alkylation of Pyrimidyl Aldehydes

Michela Quaranta,[†] Timo Gehring,[§] Barbara Odell,[||] John M. Brown,*[,||] and Donna G. Blackmond*[,†,‡,⊥]

Department of Chemistry and Department of Chemical Engineering & Chemical Technology, Imperial College London, London SW7 2AZ, United Kingdom, Institut für Organische Chemie, Karlsruher Institut für Technologie (KIT), 76131 Karlsruhe, Germany, and Chemistry Research Laboratory, Oxford University, Oxford OX1 3TA, United Kingdom

Received April 21, 2010; E-mail: blackmond@scripps.edu; john.brown@chem.ox.ac.uk

Abstract: Observations of an intriguing inverse temperature dependence on reaction rate and a profound induction period in the Soai autocatalytic reaction are reported along with detailed kinetic and NMR investigations of the product alkoxide at low temperatures, leading to the suggestion that the active catalyst is derived *in situ* from the tetrameric ground state.

The Soai autocatalytic reaction[1] (Scheme 1) stands as one of the most striking discoveries in organic chemistry of the late 20th century. Alkylation of pyrimidin-5-als with *i*-Pr_2Zn is catalyzed by some form of the zinc alkoxide product, with concurrent amplification of enantiomeric purity through a positive nonlinear effect.[2] This reaction represents the first experimental proof of concept for theoretical ideas put forward decades earlier[3] for the evolution of a single chiral state from a small imbalance of enantiomers.

Scheme 1. Soai Autocatalytic Alkylation of Pyrimidyl Aldehydes

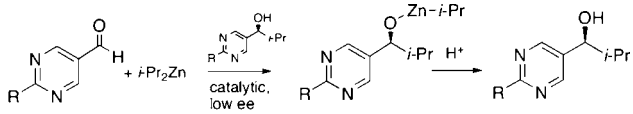

1a R = CH_3
1b R = $C_2Si(CH_3)_3$
1c R = C_2(1-adamantyl)

3 a,b,c as **1** **2** a,b,c as **1**

Blackmond and Brown reported the first mechanistic rationalization of autocatalysis with amplification of ee in the Soai reaction in 2001,[4] based on in situ monitoring of reaction progress for alkylation of aldehyde **1a** with *i*-Pr_2Zn, with **2a** employed as the precatalyst. The kinetic model developed from reaction calorimetric profiles at ambient temperature independently predicted both the temporal degree of asymmetric amplification, confirmed by compositional analysis,[4,5] as well as the relative concentrations of the catalyst species, confirmed by NMR spectroscopy.[4,6] Here we report further mechanistic studies highlighting an intriguing induction period and an inverse temperature effect on the rate of the Soai reaction. These kinetic and spectroscopic observations provide additional hints about the nature and complexity of the species in the dynamic autocatalytic network, implicating unsymmetrical and internally dynamic tetramers as the active catalyst or its immediate precursor.

Subsequent to their early publications, Soai and co-workers showed that modification of the pyrimidine 2-substituent improved reactivity and selectivity, alkynyl groups being optimal.[7] Aldehyde **1c** is a substrate recently developed by Gehring[8] that is significantly more reactive than **1a**, on which our original kinetic studies were based. The current studies are based on the **1c** reaction system, which allows systematic mechanistic studies of the Soai reaction over a wide range of conditions.

Figure 1 reveals a striking relationship between reaction temperature and reaction rate for the reaction of aldehyde **1c** in Scheme 1: the maximum reaction rate *increases* significantly as the temperature is *decreased*. This increase appears to peak at ca. 263 K, where the reaction exhibits a maximum rate more than 20-fold higher than that observed at ambient temperature.[9,10] The rate maximum for the conditions of Figure 1 occurs at ca. 36−42% conversion at all temperatures, and the form of the rate profile as a function of conversion is similar at all temperatures. The inverse relationship between rate and temperature holds for reactions over an order of magnitude of **1c** concentrations (0.01−0.1 M) using enantiopure, scalemic, or racemic **2c** as well as in reactions containing no added catalyst.[10] This trend has also been confirmed for reactions of aldehyde **1a** catalyzed by **3a**.[10]

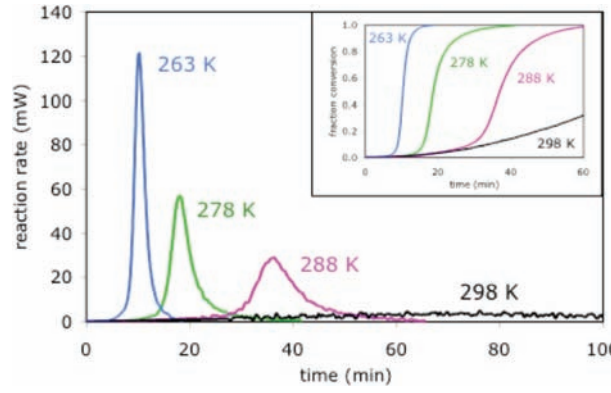

Figure 1. Kinetic profiles obtained by reaction calorimetry as a function of temperature for the reaction of substrate **1c** in Scheme 1 at different temperatures. Conditions: 0.015 M **1c**, 1.5 equiv of *i*-Pr_2Zn, and 1 mol % enantiopure **2c**. Main figure: reaction rate vs time; inset: conversion vs time. Product ee: 96−100%.

Figure 1 also reveals a significant induction period that increases in duration as reaction temperature increases (and rate decreases). This induction time to the rapid reaction phase also increases with decreasing catalyst concentration (Figure 2) and decreasing substrate concentration (Figure 3).

Interestingly, although Figure 2 shows that the reaction is not strongly dependent on the initial catalyst concentration, we found

[†] Department of Chemistry, Imperial College London.
[‡] Department of Chemical Engineering & Chemical Technology, Imperial College London.
[§] Karlsruher Institut für Technologie.
[||] Oxford University.
[⊥] Present address: Department of Chemistry, The Scripps Research Institute, La Jolla, CA 92037 USA.

 10.1021/ja103204w

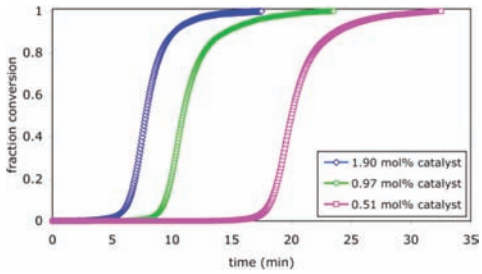

Figure 2. Conversion vs time in the reaction of Scheme 1 at 273 K for 0.015 M **1c**, 1.5 equiv of *i*-Pr_2Zn, and catalyst **3c** as in legend.

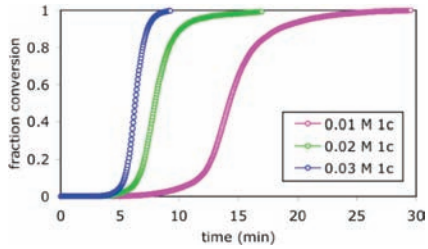

Figure 3. Conversion vs time in the reaction of Scheme 1 at 273 K for [**2c**] = 0.15 mM, 0.04 M *i*-Pr_2Zn, and initial [**1c**] as in legend.

that it is first order in product concentration as the reaction progresses (Figure 4).[10] Together with the observations of the induction period and the ensuing rate profiles, this suggests that the reaction is rapidly dominated by an active catalyst formed via reaction turnover. Reaction progress kinetic analysis of "different excess" experiments[11] reveals zero order dependence on [*i*-Pr_2Zn] and an order of 1.6 in [**1c**] (Table 1 and Figure 4). These concentration dependences hold for both enantiopure and nonenantiopure catalysts at both 298 and 273 K and are in accordance with our previous studies of the reaction of **1a**,[5a] implicating a tetrameric intermediate or transition state species. An order between 1 and 2 in aldehyde concentration suggests a transition state involving addition of one aldehyde molecule to a resting species containing a second molecule of aldehyde. Zero order dependence on [*i*-Pr_2Zn] implies either presaturation in *i*-Pr_2Zn or *i*-Pr_2Zn addition after the rate-limiting step. Reaction simulations of either model can produce the reaction orders observed here (see Supporting Information (SI)), but the latter is more consistent with previously published NMR data on alkylzinc complexation of alkoxide **3b**.[6b]

Confirming the report by Gehring,[8] we observed strong asymmetric amplification for **2c** at all temperatures (Figure 5). As has been pointed out,[6c,12] the degree of ee amplification observed with 2-alkynylpyrimidinals is higher than predicted by the dimeric catalyst model we first proposed based on kinetic and spectroscopic studies of substrate **1a**. Possible explanations for the enhanced asymmetric amplification include the involvement of higher order catalytic species or the existence of a noncatalytic tetramer, in equilibrium with the dimer catalyst, for which the heterochiral form is more stable than the homochiral form. Ercolani has argued in favor of the latter explanation.[12] NMR studies confirm, however, that racemic alkoxide **3c** shows near equal distribution between homochiral and heterochiral species at ambient temperature (45:55),[10] as we have previously reported for **3a** and **3b**.[6b]

NMR investigations on alkoxide (*S*)-**3c** help to shed light on the nature of the solution species. The aromatic region of the ^{1}H NMR spectrum of 0.025 M alkoxide (*S*)-**3c** at 298 K in C_7D_8 at 500 MHz shows significantly greater exchange broadening in the signal at 8.7 ppm, with $\omega^1/_2 = 18$ Hz compared to the previously studied analog **3b**, which showed much sharper signals at ambient

Table 1. Initial Substrate Concentrations for "Different Excess" Reaction Progress Kinetic Analysis Experiments Shown in Figure 4

entry	symbol	$[1c]_0$ (M)	$[i\text{-}Pr_2Zn]_0$ (M)	excess (M)
1	○	0.015	0.035	0.020
2	○	0.015	0.044	0.029
3	○	0.020	0.044	0.024
4	○	0.020	0.035	0.015
5	○	0.028	0.045	0.017
6	○	0.030	0.034	0.004

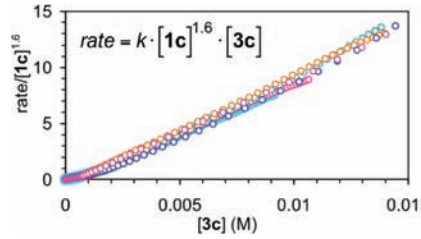

Figure 4. Reaction Progress Kinetic Analysis (RPKA) of experiments following the reaction of Scheme 1 at 273 K for [**2c**] = 0.14 mM and initial substrate concentrations and excess values given in Table 1. Overlay observed between the data plotted as rate/$[\mathbf{1c}]^{1.6}$ vs [**3c**] gives order in [**1c**] = 1.6 and order in [*i*-Pr_2Zn] = 0. Linearity gives order in [**3c**] = 1. See refs 10 and 11 for detailed descriptions of the RPKA methodology.

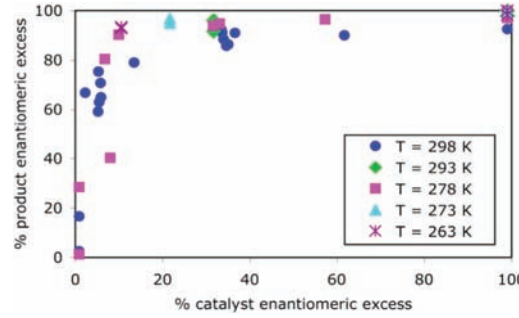

Figure 5. Product ee as a function of catalyst ee for the reaction of Scheme 1 at ca. 1 mol % **2c**; 1.5 equiv of *i*-Pr_2Zn; 0.025 M **1c** (T = 298, 278 K); 0.015 M **1c** (T = 293, 273, 263 K).

temperature, with $\omega^1/_2 = 5$ Hz.[6] On cooling, further broadening is observed, with settling of the ArH and CHO regions into discernible signals by 243 K that are sharp enough for analysis at 233 K. Figure 6 shows the low-field ROESY spectrum, demonstrating exchange processes that involve all pyrimidine proton sites. The process is comparable at high (0.1 M) and low (0.025 M) concentrations and is thus predominantly intramolecular. The lower intensity of the off-diagonal signals at 9.8 ppm indicate a slower exchange process with other pyrimidine protons. The alkoxy protons of (*S*)-**3c** in the 5−4 ppm region of the ROESY spectrum demonstrate similar behavior.

The low-field COSY-90 spectrum at 233 K shows two distinct pairs of coupled protons in the pyrimidine region between 9.8 and 8.1 ppm along with a third that is not connected to the main dynamic system. This represents an *unsymmetrical* component for which aryl rotations are restricted (presumed N−Zn coordination[13]). In addition there are four distinct strong vicinal cross-peaks observed from the $Me_2CHC\mathbf{H}OZn$ region to their respective $Me_2C\mathbf{H}CHOZn$ neighbors, along with signals indicative of further components (Figure 7). The same four C**H**OZn resonances exhibit cross-peaks in the ^{13}C HSQC spectrum and can be located in the ROESY spectrum,[10] where the NOE-derived cross-peaks with the pyrimidine region are complicated by dynamic exchange. Nevertheless, the four pyrimi-

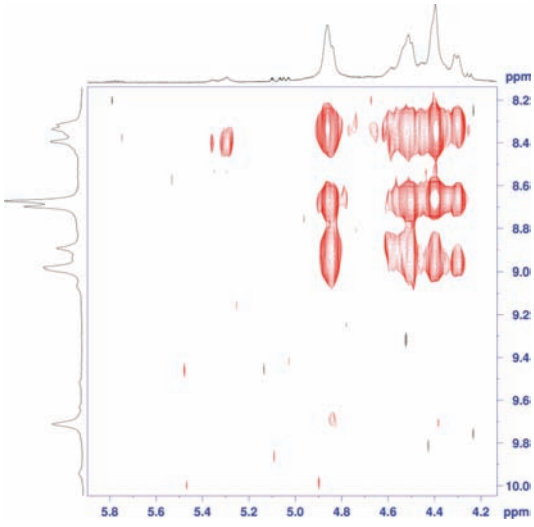

Figure 6. Low field region of the TR-ROESY spectrum of complex **3c**, 0.025 M in C_7D_8 at 233 K, with 1.1 equiv excess *i*-Pr_2Zn. The COSY-90 spectrum of the same sample (SI) shows *J*-coupling cross-peaks between signals at 9.7−8.4 ppm and between signals at 9.0−8.3 ppm.[10]

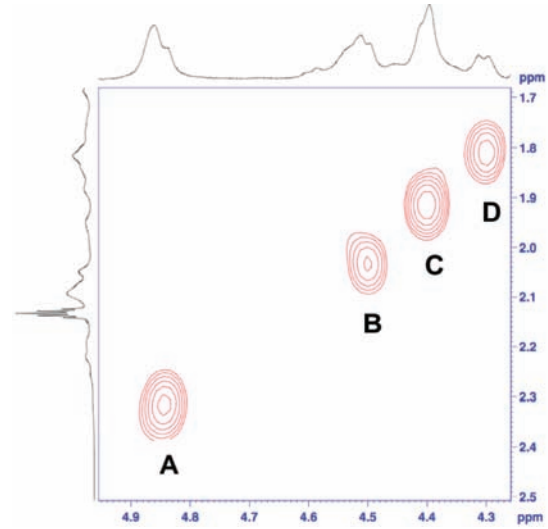

Figure 7. COSY-90 spectrum of Zn alkoxide (*S*)-**3c**, 0.025 M in C_7D_8 with 1 equiv excess *i*-Pr_2Zn at 233 K linking cross-peaks in the OC**H**CHMe$_2$ region (*x*-axis) with OCHC**H**Me$_2$ (*y*-axis).[10]

dine protons involved in COSY cross-peaks have pairwise association with alkoxide signals at 4.84 and 4.30 ppm (**A** and **D** in Figure 7). Signals **B** and **C** are linked by NOE to several peaks in the pyrimidine region, including the prominent peak at 8.67 ppm.

^{1}H DOSY spectra of alkoxide (*S*)-**3c** at 298 K and 0.025 M show that all distinct signals assigned to the alkoxide complex have comparable diffusion coefficients, $D = (4.33 \pm 0.18) \times 10^{-10}$ m^2 s^{-1} at 298 K.[10] Likewise at 233 K, the distinct signals in the 9.9−8.3 ppm region all have the same diffusion coefficient, $D = (8.60 \pm 0.12) \times 10^{-11}$ m^2 s^{-1}. To estimate the molecular weight of the aggregates formed by (*S*)-**3c** at ambient temperature and thus the degree of oligomerization, we determined diffusion coefficients for several compounds to establish an empirical calibration curve, including two reference porphyrins[10,14] and a diphosphine compound (Figure 8). Despite the fact that the molecules exhibit different shapes (and densities) our data enable us to determine the trendline $D = 2.8 \times 10^{-8} \cdot (\mathrm{RMM})^{-0.56}$. Figure 8 shows that a tetrameric Zn alkoxide (**3c**)$_4$ with an RMM of 1672 g/mol falls on this calibration line.[10] Although RMM assignment by DOSY presents challenges,[15] these measurements support the formation of a higher molecular weight aggregate from (*S*)-**3c**.[16]

The combination of COSY and ROESY spectroscopy thus permits the identification of a significant conformer containing two rotationally restricted pyrimidine rings, in dynamic equilibrium with other conformers. There is clearly more than one component present, although low temperature DOSY demonstrates comparable mobility for the individual resonances. These observations are consistent with the tetramer of SMS (square-macrocycle-square) structure, based on a macrocyclic core (Scheme 2). The involvement of tetramers and their precursors was first proposed by us in kinetic experiments[5a] and through computation,[6b,c] which suggested that the most likely tetramer structure was as shown in Scheme 2. More recently, Schiaffino and Ercolani[12] have computed a reaction pathway for autocatalysis in accord with our kinetic observations,[5] but with the macrocyclic dimer as the catalyst template leading to a barrel tetramer.

These kinetic and spectroscopic studies allow us to suggest an interpretation for the unusual inverse temperature dependence on rate observed in Figure 1. Anomalies in the well-established Arrhenius relationship between temperature and reaction rate can

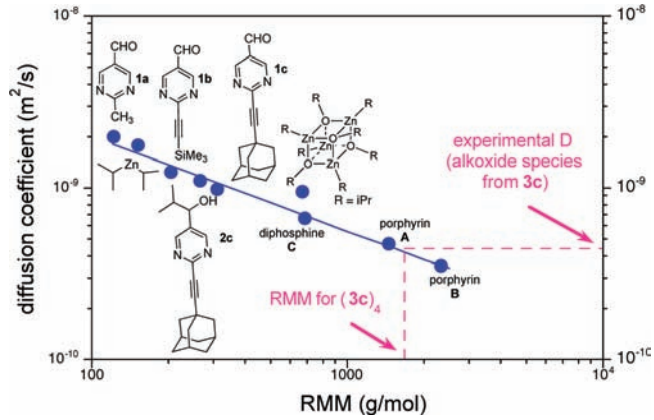

Figure 8. Diffusion coefficients as a function of RMM from ^{1}H DOSY experiments at 298 K for **1a**, **1b**, **1c**, **2c**, *i*-Pr_2Zn, (*i*-PrZnO*i*-Pr)$_4$,[14a] two reference porphyrins, and a reference diphosphine.[10,14]

Scheme 2. Proposed Structure for Homochiral Tetramer (**3c**)$_4$[17]

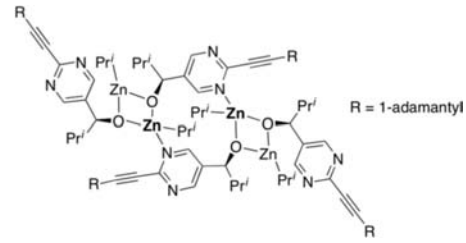

occur in multistep reactions when the different elementary steps exhibit different activation energies.[18−20] Typical cases involve stepwise chemical reactions where a shift in the rate-determining step with temperature may result in an inverse temperature dependence on rate. However, this is unlikely in our case since we found that neither the form of the kinetic profile nor the concentration dependence of the reactants is sensitive to temperature. A negative Arrhenius dependence could also result from an equilibrium between an active intermediate and an inactive species lying off the productive pathway,[18] such as might be found if the tetrameric species implicated in our kinetic and spectroscopic studies serves as both the active catalyst and the more stable partner in

equilibria with inactive species, in accordance with proposals to rationalize the observed degree of asymmetric amplification.[12]

In summary, the observation of a prolonged induction period and an unusual inverse temperature dependence on the kinetics of the Soai reaction points to the in situ formation of an active oligomeric catalyst−substrate complex that becomes increasingly stabilized as the temperature decreases. The NMR studies demonstrate a strong tendency for alkoxide (*S*)-**3c** to aggregate within the temperature region explored here by reaction kinetic studies, with preferential formation of unsymmetrical and internally dynamic tetramers at low temperature. Aggregation is maintained at ambient temperature. Further investigations are underway in our laboratories to unlock the fascinating mechanism of the Soai reaction and its implications for self-assembly, self-replication, and asymmetric amplification processes.

Acknowledgment. Preliminary experiments by Dr. J. S. Mathew are gratefully acknowledged. D.G.B. acknowledges the EPSRC and Merck for support and the Royal Society for a Wolfson Research Merit Award. J.M.B. thanks the Leverhulme Trust for a Fellowship. We thank Dr. T. D. W. Claridge for helpful comments, Dr. Chris Welch (Merck) for help with chiral HPLC, and Prof. Harry Anderson for samples. T.G. thanks M. Busch, M. Schlageter, and D. Weingand for the help in the synthesis of **1c**.

Supporting Information Available: Details of kinetic studies and NMR experiments (42 pages).This material is available free of charge via the Internet at http://pubs.acs.org.

References

(1) (a) Soai, K.; Shibata, T.; Morioka, H.; Choji, K. *Nature* **1995**, *378*, 767–768. (b) Kawasaki, T.; Matsumura, Y.; Tsutsumi, T.; Suzuki, K.; Ito, M.; Soai, K. *Science* **2009**, *324*, 492–495. (c) Soai, K.; Kawasaki, T. *Chem. Today* **2009**, *27*, 3–7. (d) For a review of experimental work on the Soai reaction, see: Gehring, T.; Busch, M.; Schlageter, M.; Weingand, D. *Chirality* **2010**, DOI: 10.1002/chir.20849.

(2) For an overview of nonlinear effects, see: Satyanarayana, T.; Abraham, S.; Kagan, H. B. *Angew. Chem., Int. Ed.* **2009**, *48*, 456–494.

(3) (a) Frank, F. C. *Biochim. Biophys. Acta* **1953**, *11*, 459–463. (b) Calvin, M. *Molecular Evolution*; Oxford University Press: Oxford, 1969.

(4) Blackmond, D. G.; McMillan, C. R.; Ramdeehul, S.; Schorm, A.; Brown, J. M. *J. Am. Chem. Soc.* **2001**, *123*, 10103–10104.

(5) (a) Buono, F. G.; Blackmond, D. G. *J. Am. Chem. Soc.* **2003**, *125*, 8978–8979. (b) Blackmond, D. G. *Proc. Natl. Acad. Sci., U.S.A.* **2004**, *101*, 5732–5736.

(6) (a) Gridnev, I. D.; Serafimov, J. M.; Quiney, H.; Brown, J. M. *Org. Biomol. Chem.* **2003**, *1*, 3811–3819. (b) Gridnev, I. D.; Serafimov, J. M.; Brown, J. M. *Angew. Chem., Int. Ed.* **2004**, *43*, 4884–4888. (c) Klankermayer, J.; Gridnev, I. D.; Brown, J. M. *Chem. Commun.* **2007**, 3151–3153. (d) Brown, J. M.; Gridnev, I. D.; Klankermayer, J. *Top. Curr. Chem.* **2008**, *284*, 35–65. (e) Gridnev, I. D.; Brown, J. M. *Proc. Natl. Acad. Sci. U.S.A.* **2004**, *101*, 5727–5731.

(7) Shibata, T.; Yonekubo, S.; Soai, K. *Angew. Chem., Int. Ed.* **1999**, *38*, 659–661.

(8) Busch, M.; Schlageter, M.; Weingand, D.; Gehring, T. *Chem.—Eur. J.* **2009**, *15*, 8251–8258.

(9) Amplifying autocatalysis is less efficient at the upper end of this temperature range.

(10) See the SI for details.

(11) (a) Blackmond, D. G. *Angew. Chem., Int. Ed.* **2005**, *44*, 4302–4320. (b) Mathew, J. S.; Klussmann, M.; Iwamura, H.; Valera, F.; Futran, A.; Emanuelsson, E. A.; Blackmond, D. G. *J. Org. Chem.* **2006**, *71*, 4711–4722.

(12) (a) Schiaffino, L.; Ercolani, G. *ChemPhysChem* **2009**, *10*, 2508–2515. (b) Schiaffino, L.; Ercolani, G. *Angew. Chem., Int. Ed.* **2008**, *47*, 6832–6835. (c) Schiaffino, L.; Ercolani, G. *Chem.—Eur. J.* **2010**, *16*, 3147–3156.

(13) Earlier ^{15}N NMR studies on **3b** prepared from ^{15}N-labeled **1b** support this suggestion (see ref 6b), the scope of the earlier work being limited by the low receptivity of ^{15}N.

(14) (a) Generated in situ: Jana, S.; Berger, R. J. F.; Frohlich, R.; Pape, T.; Mitzel, N. W. *Inorg. Chem.* **2007**, *46*, 4293–4297. (b) Taylor, P. N.; Anderson, H. L. *J. Am. Chem. Soc.* **1999**, *121*, 11538–11545.

(15) (a) Claridge, T. D. W. *High-Resolution NMR Techniques in Organic Chemistry*; Elsevier: Oxford, 2009; Chapter 9, p 303 ff. (b) Pregosin, P. S. *Prog. Nucl. Magn. Reson. Spectrosc.* **2006**, *49*, 261–288.

(16) Similarly the diffusion coefficient for (*R*)-**3b** at 298 K is $(4.8 \pm 0.08) \times 10^{-10}$ m^2 s^{-1} with an RMM value of 1423 g/mol for its tetramer.

(17) The Zn atoms labelled in bold provide additional stereogenic centers and potentially three stereoisomers in the homochiral form (This topology was first proposed by I. D. Gridnev (see ref 6e) and endorsed by DFT computation (ref 6c).

(18) (a) Cornish-Bowden, A. *Fundamentals of Enzyme Kinetics*; Portland Press Ltd: London, 1995; pp 196−197. (b) Fersht, A. *Structure and Mechanism in Protein Science: A Guide to Enzyme Catalysis and Protein Folding*, 3rd ed.; Freeman, W. H.: London, 1998.

(19) For example, see:(a) Dzudza, A.; Marks, T. J. *J. Org. Chem.* **2008**, *73*, 4004–4016 (reversible three-component pre-equilibria). (b) Moss, R. A.; Wang, L.; Zhang, M.; Skalit, C.; Krogh-Jespersen, K. *J. Am. Chem. Soc.* **2008**, *130*, 5634–5635 (entropy-controlled CCl_2 addition to alkenes). (c) Handoo, K. L.; Lu, Y.; Parker, V. D. *J. Am. Chem. Soc.* **2003**, *125*, 9381–9387 (Diels−Alder addition via reversible CT formation). (d) Bradaric, C. J.; Leigh, W. J. *J. Am. Chem. Soc.* **1996**, *118*, 8971–8972 (nucleophile addition to silaethenes via complex formation). (e) Werner, H.; Fischer, E. O.; Heckl, B.; Kreiter, C. G. *J. Organomet. Chem.* **1971**, *28*, 367–389 (fourth-order nucleophilic addition to metal−carbene complexes).

(20) (a) Peterson, M. E.; Daniel, R. M.; Danson, M. J.; Eisenthal, R. *Biochem. J.* **2007**, *402*, 331–337. (b) Oliveberg, M.; Tan, Y.-J.; Fersht, A. R. *Proc. Natl. Acad. Sci. U.S.A.* **1995**, *92*, 8926–8929.

JA103204W